ISSN 0022-4766, Journal of Structural Chemistry, 2020, Vol. 61, No. 4, pp. 574-580. © Pleiades Publishing, Ltd., 2020.
Text © The Author(s), 2020, published in Zhurnal Strukturnoi Khimii, 2020, Vol. 61, No. 4, pp. 604-610.

A NEW COORDINATION POLYMER BASED ON TWO DUAL-FUNCTIONAL LIGANDS: STRUCTURAL INSIGHTS AND TREATMENT EFFECT AGAINST INFLAMMATORY METRORRHAGIA BY INHIBITING NF-κb ACTIVATION AND IL-1β RELEASE*

H.-Y. Ren[1], L. Fu[1], and Y. Li[1]**

By the mixed-ligand approach, a new coordination polymer with the chemical formula $[Cd(bpydb)(bimb)(H_2O)](H_2O)_3$ (**1**, H_2bpydb = 4,4′-([2,4′-bipyridine]-2′,6′-diyl) benzoic acid, bimb = 5,5′-bis(1H-benzo[*d*]imidazol-2-yl)-2,2′-bipyridine) is successfully prepared via a hydrothermal reaction of $Cd(NO_3)\cdot 4H_2O$, H_2bpydb, and bimb in the presence of NaOH as the pH modulator. Furthermore, we use an ultrasonic method to obtain nanoparticles of **1** with an average thickness of 126 nm. To evaluate the anti-inflammatory effect of the compound against inflammatory metrorrhagia, the activation of NF-κb signal pathway is measured by RT-PCR. Furthermore, ELSA is used in this research to detect the IL-1β and IL-18 content.

DOI: 10.1134/S0022476620040101

Keywords: mixed-ligand, hydrothermal reaction, nanoparticles, anti-inflammatory.

INTRODUCTION

Abnormal bleeding of the endometrium is one of the most common clinical diseases of women, which is usually caused by the verification factors, such as endometrial inflammation, acute and chronic pelvic inflammatory disease, intrauterine device placement, postmenstrual hemorrhage, postpartum blood collapse, lochia, etc. [1-3]. All the factors above are directly or indirectly related to metrorrhagia inflammation. It has been reported that in abnormal endometrial hemorrhage patients, the detection rate of endometrial bacteria is high to about 80%, and the *Staphylococcus aureus* and *Escherichia coli* rank No. 1 and No. 2 of the detection rate [4, 5]. These two bacteria are considered to be the main pathogenic bacteria causing uterine inflammation.

Nuclear factor-κb (NF-κb) is a multifunctional nuclear transcription factor which is the convergence point of multiple signal pathways, which not only participates in the regulation of various gene expressions involved in inflammatory and immune responses, apoptosis and proliferation, but also participates in the development and progression of many inflammation-related diseases [6]. Now it is the most widely reported anti-inflammatory targets for clinical therapy.

[1]Department of Reproductive Medicine, Beijing Chao-yang Hospital, Capital Medical University, Beijing, P. R. China; **haiming_ren1970@126.com. Original article submitted July 8, 2019; revised September 7, 2019; accepted September 9, 2019.

* Supplementary materials are available for this article at 10.1134/S0022476620040101 and are accessible for authorized users.

Coordination polymers (CPs) are an emerging class of periodic crystalline solid-state materials constructed from metal ions or polynuclear metal–oxygen clusters and multidentate organic ligands [7-9]. In the past decades, d-block transition CPs have attracted sustainable interest not only due to their significant contributions to numerous areas, including magnetism, catalysis, gas separation, and biomedicine, but also their structural diversity and intriguing topologies [10-12]. However, the synthesis of CPs with desirable structures and properties is still arduous. A possible reason may be that crystallization is a very complicated self-assembling process in which subtle changes, such as assistant ligands, pH values, solvent systems, and reaction temperatures could have unpredictable effects on the final compositions and structures [13]. It has been previously demonstrated that the coordination nature of the metal center and the sensible choice of organic ligands are crucial factors for the target design of CPs. Many CPs have been synthesized by combining polycarboxylate anions with N-heterocyclic neutral ligands to tune their structures and properties, which show promising application in the biomedicine [14-16]. Benzimidazole is also an important constituent in several natural and synthetic compounds. It is an integral part of the structure of vitamin B12 and its broad spectrum of biological activities, such as antioxidant, antimicrobial, antiallergic, DNA binding, and anticancer, make it an important scaffold in the development of several therapeutic agents [17-19]. In this study, using the mixed-ligand approach, new CP with the chemical formula $[Cd(bpydb)(bimb)(H_2O)](H_2O)_3$ (**1**, H_2bpydb = 4,4′-([2,4′-bipyridine]-2′,6′-diyl)dibenzoic acid, bimb = 5,5′-bis(1H-benzo[*d*]imidazol-2-yl)-2,2′-bipyridine) has been successfully prepared via a hydrothermal reaction of $Cd(NO_3)\cdot 4H_2O$, H_2bpydb, and bimb in the presence of NaOH as the pH modulator. Furthermore, we used an ultrasonic method to obtain nanoparticles of **1** with the average thickness of 126 nm. Through the pharmacodynamic evaluation, we have convinced that the compound could reduce the activation of the NF-κb signal pathway by determining the relative expression of *nf*-κb and *t-pa* in endometrial epithelial cells. In addition to this, the compound could also inhibit the level of IL-1β and IL-18 detected by ELISA.

EXPERIMENTAL

Materials and instrumentation. All reagents and solvents were commercially available and used as received without further purification. Elemental analyses for C, H, and N were performed on a CHN-O-Rapid analyzer or an Elementar Vario MICRO analyzer. IR spectra were recorded with a Thermo Scientific Nicolet 5700 FTIR spectrophotometer in KBr pellets from 400 cm^{-1} to 4000 cm^{-1}.

Synthesis of $[Cd(bpydb)(bimb)(H_2O)](H_2O)_3$ (1). A mixture of $Cd(NO_3)_2\cdot 4H_2O$ (0.0154 g, 0.05 mmol), H_2bpydb (0.039 g, 0.1 mmol), bimb (0.019 mg, 0.05 mmol), NaOH (10 mg), and H_2O (5 mL) was sealed in a 15 mL Teflon-lined stainless-steel autoclave under autogenous pressure, heated at constant 120 °C for 3 days, and then slowly cooled to room temperature. Light yellow block crystals of **1** were collected by filtration, successively washed with H_2O and EtOH, and dried in air, with a yield of 68% based on the bimb ligand. Elem. anal. Calc. for **1** ($C_{48}H_{38}CdN_8O_8$): C 59.60, H 3.96, N 11.58. Found for **1**: C 59.72, H 4.04, N 11.71.

Synthesis of nanosized $[Cd(bpydb)(bimb)(H_2O)](H_2O)_3$ (1). H_2bpydb (0.039 g, 0.1 mmol) and bimb (0.019 mg, 0.05 mmol) were poured into a 10 mL water solution of 0.057 g (1 mmol) cadmium(II) acetate and 10 mg of NaOH under ultrasound irradiation. Two distinct ultrasonic baths were used with different powers (138 W and 305 W) for 1 h respectively. A large amount of nanosized compound **1** was obtained.

Crystal structure and refinement. The structure data on complex **1** were collected on a Super Nova diffractometer equipped with CuK_α (λ = 1.5406 Å) and an Atlas CCD detector. These structures were resolved by direct methods and refined by the full-matrix least squares fitting on F^2 using the SHELX-2016 software package [20]. All non-hydrogen atoms were refined with anisotropic thermal parameters except the solvent molecules. Hydrogen atoms on the aromatic rings were located at geometrically calculated positions and refined by the riding model. A summary of the crystallographic parameters and refinement results are listed in Table 1.

TABLE 1. Structural Parameters and Refinement Indices for Complex **1**

Parameter	**1**
Empirical formula	$C_{48}H_{32}CdN_8O_5$
Formula weight	913.21
Temperature, K	293(2)
Crystal system	Monoclinic
Space group	$P2_1/c$
a, b, c, Å	16.918(2), 27.418(3), 12.3595(14)
β, deg	122.128(7)
V, Å^3	4855.1(11)
Z	4
ρ_{calc}, g/cm^3	1.249
μ, mm^{-1}	0.500
Reflections collected	8981
No. unique data [R(int)]	8981 [0.000]
No. data with $I \geq 2\sigma(I)$	2[illegible]9
R_1 / wR_2 (all data)	0.0888 / 0.[illegible]64
CCDC	[illegible]939091

RT-PCR detection. The activation the NF-κb signal pathway after compound treatment was detected by RT-PCR according to manufacture′s protocols with a little modification. In short, the endometrial epithelial cells in the logarithmic growth phase were collected and seeded into 6 well-plates at the destiny of $1\cdot10^5$ cell/well, placed and cultured at 37 °C, 5% CO_2 condition for 12 h to get 70-80% confluence. 2 μg/mL LPS was added into cells for pre-treatment, followed by the compound addition for further treatment at the concentration of 5 μg/mL. After treatment, the endometrial epithelial cells in different groups were all collected for RNA extraction with manufacture′s kit. The RNA sample was quantified with a spectrophotometer and then reverse transcripted into cDNAs with cDNA Reverse Transcription Kit. RT-PCR was performed to detect the relative expression of *nf*-κb and the tissue plasminogen activator (*t-pa*); *gapdh* was used as the internal reference in this experiment. The relative expression level of *nf*-κb and *t-pa* genes was calculated according to the $2^{-\Delta\Delta Ct}$ method. This experiment was performed in triplicate.

ELISA assay. IL-1β and IL-18 inflammatory cytokines are the downstream production of the NF-κb signal pathway. When the NF-κb signal pathway is activated, there is usually a significantly increased level of IL-1β and IL-18. In this experiment, after compound treatment, by ELISA it was determined whether the content of inflammatory cytokines could be affected or not. In brief, the endometrial epithelial cells were incubated with LPS and then treated with the compound. The cell supernatant was collected and the content of IL-1β and IL-18 was measured using the ELISA detection kit according to the instructions. This experiment was performed at least three times.

RESULTS AND DISCUSSION

Structural description of compound 1. The single crystal data analysis reveals that complex **1** crystallizes in a 1D chain structure with the monoclinic crystal system, space group $P2/c$. The asymmetric unit of **1** consists of one N-donor ligand, one L^{2-}, and one central Cd(II) ion. As shown in Fig. 1*a*, the seven-connected central Cd(II) ion is coordinated by four O atoms of two carboxyl groups from two different L^{2-} ligands, two N atoms from one N-donor ligand, and one aqueous atom. The Cd–N bond distances are in the range from 2.3088(2) Å (Cd1–N3) to 2.3437(2) Å (Cd1–N4), and the Cd–O bond lengths are in the range from 2.2160(2) Å (Cd1–O1) to 2.6291(4) Å (Cd1–O2, Table 2). They are comparable with other Cd-based CPs based on N-donor and O-donor co-ligands [21, 22]. As shown in Fig. 1*b*, the two carboxyl groups of one fully

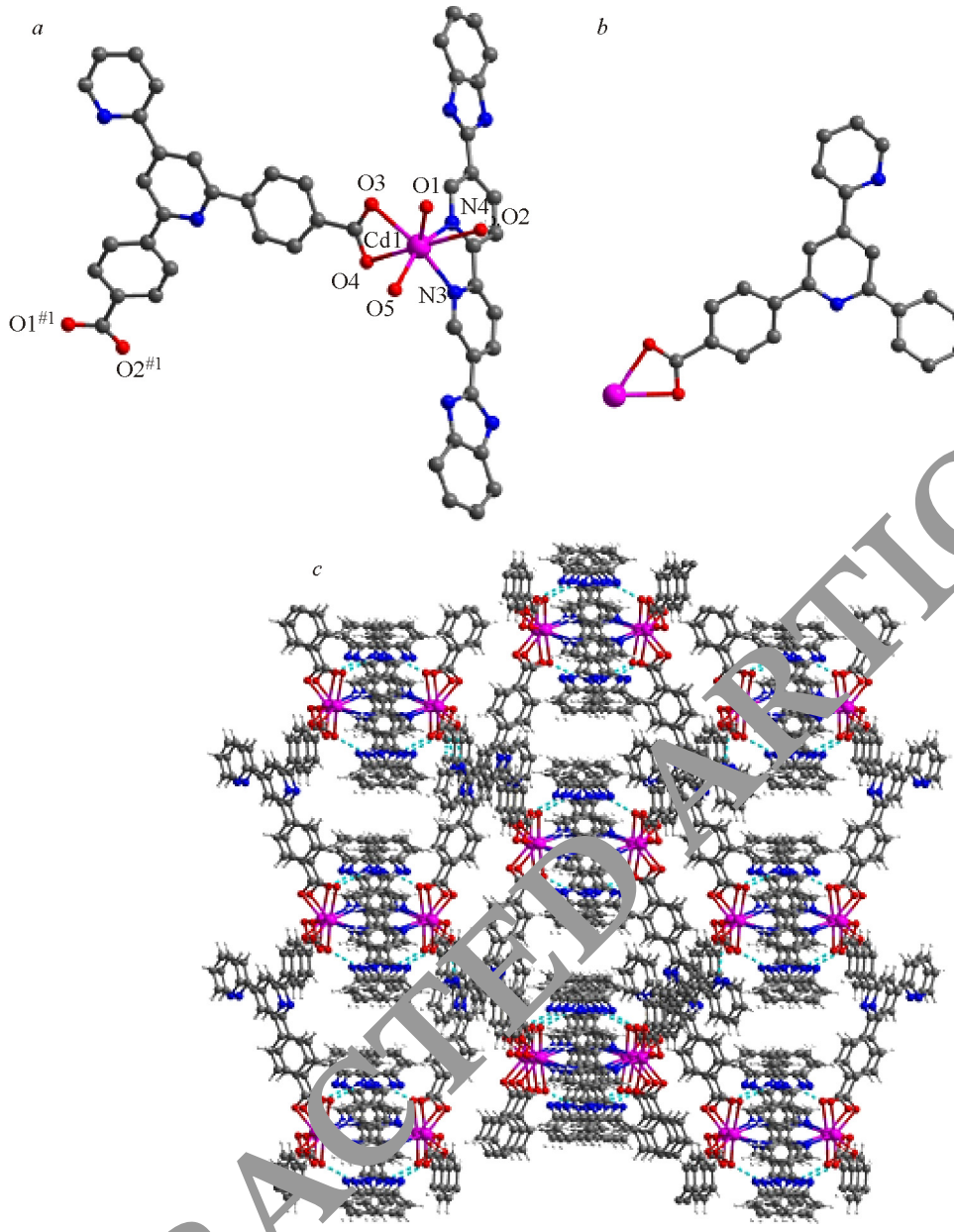

Fig. 1. The coordination environment of central Cd(II) ions in **1** (*a*). The symmetry code: #1 1+*x*, *y*, *z*; the bidentate coordination mode with L^{2-} (*b*); the supramolecular structure of **1** connected by H-bonds (*c*).

TABLE 2. Selected Bond Lengths (Å) for **1**

Bond	Length, Å	Bond	Length, Å
Cd1—N3	2.309(7)	C9—C14	1.384(12)
Cd1—N4	2.342(7)	C10—C11	1.394(10)
Cd1—O1	2.213(7)	C11—C12	1.350(10)
Cd1—O2	2.627(7)	C12—C13	1.382(12)
Cd1—O3	2.405(5)	C12—C19	1.471(11)
Cd1—O4	2.360(6)	C13—C14	1.408(11)
Cd1—O5	2.313(5)	C15—C16	1.394(10)
Cd1—C8	2.677(10)	C16—C17	1.352(11)

depronated L^{2-} ligand adopt the bidentate chelating coordination mode with two Cd(II) ions, which produces a 1D chain structure (Supplementary Materials Fig. S1*a*). The N-donor ligand adopts the chelating coordination mode with the Cd(II) center, which hinders the further extend of the structure, giving a 1D chain structure in **1** (Fig. S1*b*). In addition, the adjacent 1D chains are further connected with each other into a supramolecular structure via the O(5)–H(5A)…N(2), N(6)–H(6)…O(3), and N(8)–H(8)…O(2) H-bonds (Fig. 1*c*). The detailed information of the hydrogen bonding is given in Table 3.

Preparation of the nanostructure of 1. Considering the following bioactivity tests, the reagents are required not only to have a high bioactivity, but also are hoped to be in nanoscale, which facilitates the release of drugs to the whole body and absorption by the specific tissues at intravenous administration. Nano CPs possess several advantageous features over existing nanosystems, such as the size, shape, and composition of nano CPs could be easily tuned via synthetic manipulations, they are highly porous and oriented structures for efficient loading properties, etc. Moreover, nano CPs are intrinsically biodegradable since the metal–ligand bonds are labile in nature and thus could be easily excreted from the system after its bio function. Nanostructured **1** has been synthesized in the nanocrystalline form by the addition of reagents in ultrasonic baths with different powers. The formation of nano **1** has been further confirmed by scanning electron microscopy (SEM) studies obtained by drop-casting a DMSO-dispersed solution of nano **1** on a glass surface. It shows that nano **1** has a rod-like morphology with the average thickness distribution of around 126 nm, with all rods being arranged in parallel (Fig. 2).

Compound reduced relative expression of *nf*-κb and *t-pa* in endometrial epithelial cells. NF-κb is important in the cell physiological process, which could regulate the cell inflammatory and immune response, apoptosis and proliferation, and it has been one of the most widely reported targets for inflammatory diseases therapy. During inflammatory disease, the local tissues could produce a large amount of *t-pa* to damage the normal cells around it; *t-pa* is also an important indicator for the evaluation of the inflammatory level. Thus, in this experiment, the level of *nf*-κb and *t-pa* was determined by RT-PCR. As the results show (Fig. 3), LPS treatment significantly increased the level of *nf*-κb and *t-pa* in endometrial epithelial cells, reflecting a very high inflammatory level in the model group as compared with control groups. However, after treating with the compound, the *nf*-κb and *t-pa* expression level was obviously reduced nearly to the normal level.

TABLE 3. Hydrogen Bond Geometry (Å, deg) for Compound **1**

D–H···A	D–H	H···A	D···A	D–H···A
O(5)–H(5A)···N(2)	0.85	2.02	2.841(13)	164
N(6)–H(6)···O(3)	0.85	2.01	2.818(9)	157
N(8)–H(8)···O(2)	0.86	1.85	2.694(14)	165

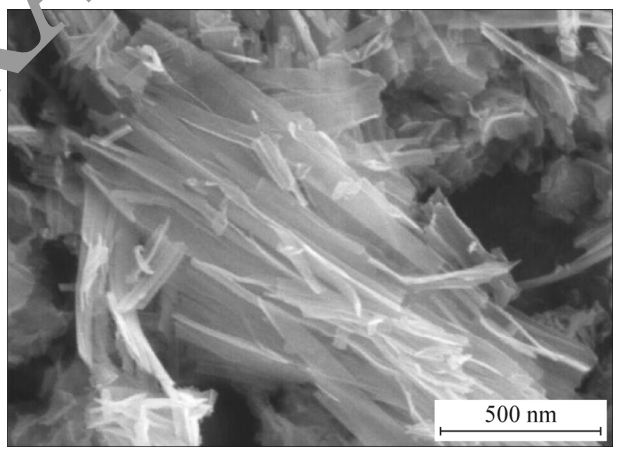

Fig. 2. The SEM diagram for the nano **1**.

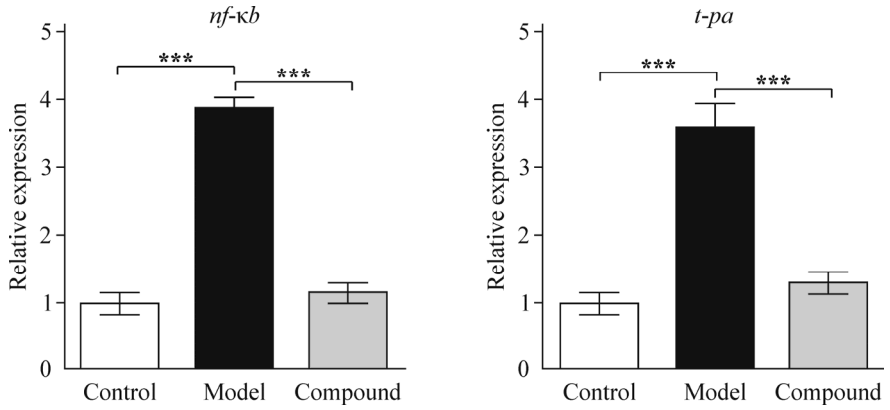

Fig. 3. Reduced *nf-κb* and *t-pa* in endometrial epithelial cells after compound treatment. The endometrial epithelial cells were stimulated with LPS and then treated with the compound, the relative expression of *nf*-κb and *t-pa* in mRNA was measured by RT-PCR. Data were showed as mean±SD.

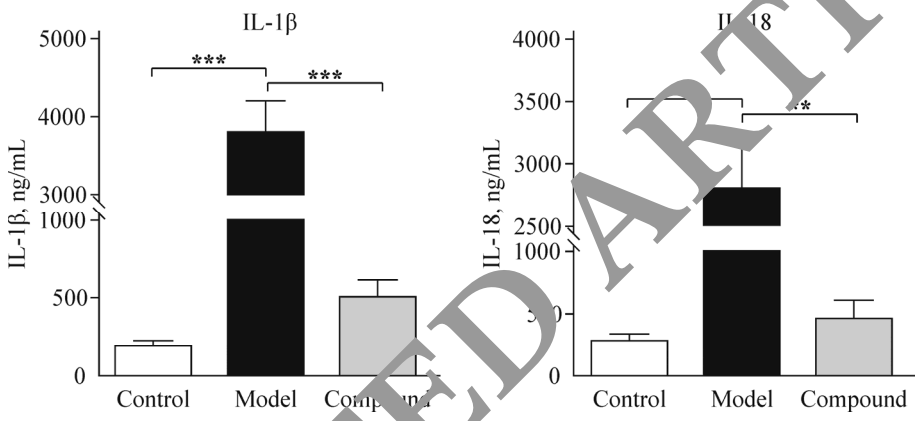

Fig. 4. Reduced IL-1β and IL-18 level in endometrial epithelial cells after the compound treatment. The endometrial epithelial cells were stimulated with LPS and then treated with the compound; the cell supernatant was collected and the content of IL-1β and IL-18 was measured using the ELISA detection kit. This experiment was repeated at least three times.

Compound inhibited content of IL-1β and IL-18. As the production of NF-κb signal pathway, IL-1β and IL-18 levels would be up-regulated when there is a high inflammatory level. In the previous study, we have convinced that the compound could reduce the increased inflammatory level induced by LPS, therefore in this experiment, we performed the ELISA assay also to prove this phenomenon. From the results in Fig. 4, we can see LPS significantly promote the expression of IL-1β and IL-18, which is consistent with the previous study, and the compound treatment reversed this up-regulation. After the compound treatment, the level of IL-1β and IL-18 was back to almost normal level, which has no difference with the control group. This study confirmed that the compound could reduce the inflammatory state.

CONCLUSIONS

In summary, we have successfully prepared new Cd(II)-based CP by applying the mixed-ligand approach. The chemical composition of as-prepared complex **1** has been determined via the elemental analysis and the structural arrangement has been probed via single crystal X-ray diffraction, which revealed that complex **1** has a 1D chain-like structure based on seven-coordinated Cd(II) centers. Furthermore, we used an ultrasonic method to obtain nanoparticles of **1** with the average thickness of 126 nm. In the biological study, to develop a novel candidate for endometrial inflammatory disease, the

endometrial epithelial cells were treated with the compound followed by the LPS stimulation. The activation of the NF-κb signal pathway was measured by RT-PCR. The results indicated that the compound could reduce the activation of the NF-κb signal pathway. The IL-1β and IL-18 content detected by ELISA revealed the inhibition effect of the compound on the inflammatory levels of endometrial epithelial cells.

CONFLICT OF INTERESTS

The authors declare that they have no conflict of interests.

REFERENCES

1. N. Makris, G. Iatrakis, G. Sakellaropoulos, A. Rodolakis, and S. Michalas. *Clin. Exp. Obstet Gynecol.*, **2000**, *27*, 27.
2. P. Brzezinski, S. J. Gulin, D. Gulin, and A. Chiriac. *Indian J. Pharmacol.*, **2017**, *49*, 470.
3. D. Zhang, H. Q. Zhang, S. Zhao, Z. G. Li, and S. X. Hou. *Int. J. Electrochem. Sci.*, **2019**, *14*, 1659.
4. J. F. Zaldivar-Jolissaint, D. Bervini, M. Morisod Harari, and D. Baud. *Lancet*, **2015**, *385*, 68.
5. L. Kang, L. Zhao, S. Yao, and C. Duan. *Ceram. Int.*, **2019**, *45*, 16717.
6. L. Bricaire, E. Laroche, and S. Christin-Maitre. *Arch. Pediatrie*, **2013**, *20*, 910.
7. Y. Y. Yang, L. Kang, and H. Li. *Ceram. Int.*, **2019**, *45*, 8017.
8. C. Duan, J. Huo, F. Li, M. Yang, and H. Xi. *J. Mater. Sci*., **2018**, *53*, 16276.
9. L. Zhao, L. Kang, and S. Yao. *IEEE Access*, **2019**, *7*, 984.
10. X. Feng, B. Liu, L. Y. Wang, J. S. Zhao, J. G. Wang, N. S. Weng, and X. G. Yi. *Dalton Trans.*, **2010**, *39*, 8038.
11. X. Feng, R. Li, and L. Wang. *CrystEngComm*, **2015**, *17*, 7878.
12. X. Feng, C. Xu, Z. Wang, S. Tang, W. Fu, B. Ji, and L. Y. Wang. *Inorg. Chem.*, **2015**, *54*, 2088.
13. M. Rancan and L. Armelao. *Chem. Commun.*, **2015**, *51*, 12417.
14. S. Mukherjee, S. Ganguly, K. Manna, S. Mondal, S. Mahapatra, and D. Das. *Inorg. Chem.*, **2018**, *57*, 4050.
15. D. S. Raja, N. S. P. Bhuvanesh, and K. Natarajan. *Dalton Trans.*, **2012**, *41*, 4365.
16. A. M. Spokoyny, D. Kim, A. Sumrein, and C. A. Mirkin. *Chem. Soc. Rev.*, **2009**, *38*, 1218.
17. B. Can-Eke, M. O. Puskullu, E. Buyukbingol, and M. Iscan. *Chem. Biol. Interact.*, **1998**, *113*, 65.
18. S. Grassman, B. Sadek, X. Lignea, S. Elz, C. R. Ganellin, J. M. Arrang, J. C. Schwartz, H. Stark, and W. Schunack. *Eur. J. Pharm. Sci.*, **2002**, *12*, 367.
19. C. Beaulieu, Z. Wang, D. Denis, S. Greig, S. Lamontagne, G. O′Neill, D. Slipetz, and J. Wang. *Bioorg. Med. Chem. Lett.*, **2004**, *14*, 3195.
20. G. M. Sheldrick. *Acta Crystallogr., Sect. C: Struct. Chem.*, **2015**, *71*, 3.
21. D. M. Chen and X. J. Zheng. *CrystEngComm*, **2019**, *21*, 4696.
22. S. L. Cai, L. Lu, Y. P. Wu, J. Wang, Y. C. Sun, A. Q. Ma, A. Singh, and A. Kumar. *Inorg. Chim. Acta*, **2019**, *484*, 291.